New Inorganic-Based Drug Delivery System of Indole-3-Acetic Acid-Layered Metal Hydroxide Nanohybrids with Controlled Release Rate

Jae-Hun Yang,[†,‡] Yang-Su Han,[†] Man Park,[§] Taeun Park,[†] Seong-Ju Hwang,[†] and Jin-Ho Choy*[,†]

Center for Intelligent Nano-Bio Materials (CINBM), Division of Nano Sciences and Nanohybrid Co. Ltd., Ewha Womans University, Seoul 120-750, Korea, Department of Chemistry, BK-21 School of Chemical Materials Science, and SKKU Advanced Institute of Nanotechnology, Sungkyunkwan University, Suwon 440-746, Korea, and Division of Applied Biology and Chemistry, Kyungpook National University, Taegu 702-701, Korea

Received January 27, 2007. Revised Manuscript Received March 19, 2007

We have developed new inorganic-based drug delivery systems through the hybridization of indole-3-acetic acid (IAA) and layered metal hydroxide such as zinc basic hydroxide salt (ZBS) and zinc aluminum layered double hydroxide (ZALDH). A coprecipitation method as well as an ion-exchange route is found to be commonly effective in synthesizing both IAA-ZBS and IAA-ZALDH nanohybrids, in which the tilted bilayers of IAA are stabilized in the interlayer space of layered metal hydroxide lattice. According to the FT-IR spectroscopic analyses, IAA molecules interact more strongly with the ZBS lattice than the ZALDH one, which is due to the formation of coordination bonds between carboxyl groups of the guest species and coordinatively unsaturated $Zn(OH)_3$ units of the host ZBS lattice. Such an interaction gives rise to a slower release of the IAA molecules from the ZBS-based nanohybrid than from the ZALDH-based one. The present results underscore that the layered hydroxydouble salt like ZBS makes it possible to design and develop new efficient drug-delivery systems with the suspended release of guest molecules.

Introduction

Recently, intense research interests have paid on layered inorganic solids because of their ability to encapsulate and immobilize various bio- and organic molecules in the interlayer space.[1−5] In particular, layered double hydroxide (LDH) with brucite-type lattice can act as a gene reservoir and/or a drug-delivery system (DDS).[3,4,6−11] The positive surface charge of LDH layer caused by the partial substitution of divalent cations with trivalent ones makes it possible to intercalate negatively charged drug- or biomolecules like DNA. For the practical use of LDH as a drug delivery vector, it is very important to control the release rate of drug molecules,[11] because it determines the retention time of drug molecules in vivo. Such a regulation of the disintercalation kinetics of intercalated organic molecules can be achieved by tuning the chemical interaction between host and guest. It has been well-known that metal vacancy in the brucite-like layer leads to the phase transformation into hydroxy-double salt (HDS) such as $Zn_5OH_8(NO_3)_2{\cdot}2H_2O$, in which coordinatively unsaturated $Zn(OH)_3$ units are formed up and down side of vacant octahedral sites of brucite-like layers, and exposed to the interlayer space of the HDS lattice. Like the LDH phase, there are exchangeable interlayer anionic species in the HDS lattice to neutralize the positive charge of host layer and hence this material has an ability to form the intercalation complexes with negatively charged organic molecules.[12−15] The presence of the coordinatively unsaturated $Zn(OH)_3$ units directed to interlayer space allows the HDS phase to strongly interact with guest molecules. In this regard, it is highly feasible that the intercalation of drug molecules into the HDS phase would produce new inorganic-based DDS with slow release kinetics of guest drug molecules. Moreover, the HDS phase has an additional advantage over the LDH phase such as a greater capacity to accommodate guest molecules caused by its higher charge

* To whom correspondence should be addressed. Tel: 82-2-3277-4135. Fax: 82-2-3277-4340. E-mail: jhchoy@ewha.ac.kr.
† Ewha Womans University.
‡ Sungkyunkwan University.
§ Kyungpook National University.

(1) Atwood, J. L.; Davies, J. E. D.; MacNicol, D. D.; Vögtle. F. *Comprehensive Supramolecular Chemistry, Vol 7, Solid-State Supramolecular Chemistry: Two- and Three-Dimensional Inorganic Networks*, 1st ed.; Pergamon: Oxford, U.K., 1996.
(2) Yang, J. H.; Lee, S. Y.; Han, Y. S.; Park, K. C.; Choy, J. H. *Bull. Kor. Chem. Soc.* **2003**, *24*, 499.
(3) Choy, J. H.; Kwak, S. Y.; Park, J. S.; Jeong, Y. J. *Angew. Chem., Int. Ed.* **2000**, *39*, 4042.
(4) Choy, J. H.; Kwak, S. Y.; Park, J. S.; Jeong, Y. J.; Portier, J. *J. Am. Chem. Soc.* **1999**, *121*, 1399.
(5) Hussein, M. Z. B.; Long, C. W. *Mater. Chem. Phys.* **2004**, *85*, 427.
(6) Choy, J. H.; Jung, J. S.; Oh, J. M.; Park, M.; Jeong, J. Y.; Kang, Y. K.; Han, O. J. *Biomater.* **2004**, *23*, 3059.
(7) Choy, J. H.; Kwak, S. Y.; Park, J. S.; Jeong, Y. J. *J. Mater. Chem.* **2001**, *11*, 1671.
(8) Hwang, S. H.; Han, Y. S.; Choy, J. H. *Bull. Kor. Chem. Soc.* **2001**, *22*, 1019.
(9) Khan, A. I.; O'Hare, D. *J. Mater. Chem.* **2002**, *12*, 3191.
(10) Ambrogi, V.; Fardella, G.; Grandolini, G.; Perioli, L. *Int. J. Pharm.* **2001**, *220*, 23.
(11) Williams, G. R.; O'Hare, D. *J. Mater. Chem.* **2006**, *16*, 3065.
(12) Stahlin, W.; Oswald, H. R. *Acta Crystallogr., Sect. B* **1970**, *26*, 860.
(13) Newman, S. P.; Jones, W. J. *Solid State Chem.* **1999**, *148*, 26.
(14) Meyn, M.; Beneke, K.; Lagaly, G. *Inorg. Chem.* **1993**, *32*, 1209.
(15) Kandare, E.; Hossenlopp, J. M. *J. Phys. Chem. B* **2005**, *109*, 8469.

10.1021/cm070259h CCC: $37.00
Published on Web 04/20/2007

Table 1. Contents of IAA, Cationic Ratios, and Chemical Compositions of the ZBS- and ZALDH-Based Nanohybrids

	content of IAA (wt %)[a]	Zn/Al molar ratio[b]	chemical composition[c]
IAA−ZBSI	42.3		$Zn_5(OH)_8(IAA)_2{\cdot}1.5H_2O$
IAA−ZBSC	41.2		$Zn_5(OH)_8(IAA)_2{\cdot}1.9H_2O$
IAA−ZALDHI	30.7	2.1	$Zn_{0.68}Al_{0.32}(OH)_2[(IAA)_{0.26}(CO_3)_{0.03}]0.7H_2O$
IAA−ZALDHC	34.5	2.03	$Zn_{0.67}Al_{0.33}(OH)_2[(IAA)_{0.30}(NO_3)_{0.03}]0.6H_2O$

[a] Calculated from HPLC analysis. [b] Calculated from ICP data. [c] Calculated from CHN analysis, ICP, TGA-DTA data.

density.[16] Recently our group reported the synthesis of several intercalation complexes of HDS.[2,8] To date, however, no systematic studies have been carried out on the preparation and characterization of an HDS-based drug-delivery vector. Instead, most studies dealing with the intercalation chemistry of HDS or LDH have been concentrated on the applications as catalysts and catalyst supports, adsorbents, ceramic precursors, and inorganic matrices.[17−22]

In the present study, we have synthesized new HDS-based DDS in which indole-3-acetic acid (IAA) molecules are stabilized in the interlayer space of $Zn_5(OH)_8(NO_3)_2{\cdot}2H_2O$ (ZBS). For comparison, we have also prepared the hybrid compounds consisting of IAA and LDH ($Zn_2Al(OH)_6(NO_3){\cdot}xH_2O$, ZALDH). We have chosen IAA as a guest molecule not only because it is very unstable to the oxygen atmosphere and UV−vis irradiation, but also because it has high potentials as a prodrug and a cosmetic or dermatological ingredient.[23−27] The obtained nanohybrids have been comparatively investigated in order to probe the effect of host lattice on the chemical bonds between host and guest and the disintercalation kinetics of the guest IAA.

Experimental Section

Synthesis. The hybridization of IAA ($C_{10}H_9NO_2$, Lancaster; England) with inorganic layered compounds was achieved by both ion exchange and coprecipitation reactions at room temperature.[2,8] For the synthesis through the ion-exchange reaction, the pristine ZBS was prepared by adjusting the pH of aqueous 0.4 M $Zn(NO_3)_2{\cdot}6H_2O$ solution to 7.0 (± 0.1) with 1 M NaOH solution, whereas the pristine ZALDH was obtained by titrating 2 M NaOH solution into the aqueous mixture solution of 1 M $Zn(NO_3)_2{\cdot}6H_2O$ and 0.5 M $Al(NO_3)_3{\cdot}9H_2O$ up to pH = 8.0 (± 0.1). The resulting precipitates were aged for 12 h, washed thoroughly with decarbonated water, and dried under a vacuum. The ion-exchange process between IAA and the pristine compounds (hereafter denoted as IAA-ZBSI and IAA-ZALDHI) was done as follows: 90 mL of 0.2 M IAA solution corresponding to ~3× excess anion exchange capacity of the pristine materials was added into a decarbonated water suspension of ZBS or ZALDH powders (2 wt % 100 mL) at pH = 7 (± 0.1) under vigorous stirring.[28,29] After 24 h of ion-exchange reaction, the resulting products were thoroughly washed with the mixed solution of ethanol and decarbonated water (1:1 in a volume ratio) to remove the remaining nitrate and IAA ions and then vacuum-dried. Coprecipitation method was also employed to prepare the IAA hybrids. The IAA-ZBS hybrid (hereafter denoted as IAA-ZBSC) was prepared by adding 1 M $Zn(NO_3)_2{\cdot}6H_2O$ solution into a 0.25 M IAA ethanol solution at the fixed pH of 7.0 (± 0.1) under vigorous stirring. The IAA-ZALDH hybrid (hereafter denoted as IAA-ZALDHC) was obtained by adding 100 mL of an aqueous solution of 1 M $Zn(NO_3)_2{\cdot}6H_2O$ and 0.5 M $Al(NO_3)_3{\cdot}9H_2O$ into a 100 mL ethanol solution of 0.75 M IAA at a pH of 8.0 (±0.2) under vigorous stirring. The resultant white precipitates were aged for 12 h, washed, and dried under a vacuum. To prevent the carbonate contamination of the products from water solvent and ambient atmosphere, we prepared all of the aqueous solutions with decarbonated water and, during the reaction, nitrogen gas was purged into the reactant solution for all of the synthesis procedures described here. Also, the photodegradation of the IAA compound was carefully avoided by protecting the reactors from UV−vis irradiation.

Characterization. Powder X-ray diffraction (XRD) patterns were measured with a Philips PW 1830 diffractometer with Ni-filtered Cu Kα radiation (λ = 1.5418 Å) from the thin film of the samples deposited on glass substrate. Field emission-scanning electron microscopic (FE-SEM) image was monitored with a Hitachi S-4300. To avoid the influence of local charging and heating, the powder samples were coated with conductive Pt−Pd metal for 150 s in vacuum. Fourier-transformed infrared (FT-IR) spectra were collected with a JASCO FT/IR-660 plus spectrophotometer. As listed in Table 1, the compositions of the hybrids were determined from elemental CHN analyses with EA1110 (CE instrument, Italy) and inductive coupled plasma (ICP) analyses with Shimadzu ICPS-1000IV, respectively. A simultaneous thermogravimetric analysis-differential thermal analysis (TGA-DTA) for the hybrids was performed under an ambient atmosphere at a heating rate of 5 °C/min with Rigaku TAS-100 thermal analyzer. To determine the content of IAA, all the powder samples were dissolved in the mixed solution of 0.1 M HCl aqueous solution and acetonitrile (0.1 M HCl:acetonitrile = 40:60 in a volume ratio) to recover pure IAA molecules from hybrids and filtered with a 0.2 μm PTFE filter.

(16) The layer charge of the LDH phase is created by the partial replacement of divalent metal ions with trivalent one, leading to the introduction of positive charges in the host lattice. In the case of the ZBS phase, the introduction of Zn^{2+} vacancy in the brucite lattice introduces two holes per each cation vacancy. Taking into account the substituted rate of the LDH phase (33% for 2:1 type and 25% for 3:1 type) and the population of cation vacancy in the HDS phase (25% of metal sites in the brucite lattice), the charge density of the latter is generally greater than that of the former.

(17) Choudary, B. M.; Kantam, M. L.; Rahman, A.; Reddy, Ch. V.; Rao, K. K. *Angew. Chem., Int. Ed.* **2001**, *40*, 763.
(18) Hibino, T.; Tsunashima, A. *Chem. Mater.* **1997**, *9*, 2082.
(19) Millange, F.; Walton, R. I.; Lei, L.; O'Hare, D. *Chem. Mater.* **2000**, *12*, 1990.
(20) Nunan, J. G.; Himelfarb, P. B.; Herman, R. G.; Kler, K.; Bogdan, C. E.; Simmons, G. W. *Inorg. Chem.* **1989**, *28*, 3868.
(21) Alejandre, A.; Medina, F.; Salagre, P.; Correig, X.; Sueiras, J. E. *Chem. Mater.* **1999**, *11*, 939.
(22) Narita, E.; Pkaviratna, P. D.; Pinnavaia, T. J. *Chem. Commun.* **1993**, 60.
(23) Chndramohan, G.; Kalyanasundgaram, S.; Renganathan, R. *Int. J. Chem. Kinet.* **2002**, *34*, 569.
(24) Karbownik, M.; Gitto, E.; Lewinski, A.; Reiter, R. J. *J. Cell. Biochem.* **2001**, *81*, 693.
(25) Song, J.; Koch, J.; Sdquier; M. U.S. Patent 6 174 541 B1, Jan. 16, 2001.
(26) Breton, L.; Girerd, F.; Renault, B. U.S. Patent 6 521 239 B1, Feb. 18, 2003.
(27) Folkes, L.K.; Wardman, P. *Biochem. Pharm.* **2001**, *61*, 129.

(28) Taking into account the fact that IAA is a weak acid with pK_a of 4.75 (ref 29), we have carried out the hybridization reaction at pH >6 in which IAA is completely deprotonated and intercalated into the positively charged interlayer surface of ZBS or ZALDH.

(29) Budavari, S.; O'Neil, M. J.; Smith, A.; Heckelman, P. E.; Kinneary, J. F. *The Merck Index*, 12th ed.; Merck & Co., Inc.: Whitehouse Station, NJ, 1996.

The content of IAA was determined by high performance liquid chromatography (HPLC) spectra with an Agilent 1100 series Instrument equipped with a UV detector ($\lambda_{max} = 280$ nm). An octadecyl-silica reversed-phase column (4.6 × 250 mm, Zorbax) and a mobile phase containing an aqueous 0.1 M K_2HPO_4 solution at pH 4.5 and acetonitrile in the volume ratio of 55:45 were used with a flow rate of 1 mL/min and 10 μL of injection volume.

Measurements of IAA Release Rate and Chemical Stability. The release behavior of the encapsulated IAA from the hybrids was profiled in a dilute solution of sodium chloride, which is very similar to the body fluid condition. IAA-ZBS powder (253 mg) or IAA-ZALDH powder (320 mg) were dispersed in the mixed solution of 450 mL of 0.08 wt % NaCl solution and 50 mL of ethanol and stirred at 32 °C with a rate of 50 rpm. The amount of released IAA was determined periodically by monitoring the variation of absorbance peak at $\lambda = 280$ nm (λ_{max} of IAA). To understand the kinetics for the release behavior of IAA from the hybrids, we have tried to fit the measured data with following several kinetic models.[30−34]

(1) A first-order rate model has been applied extensively to the ion exchange reaction or release process and can be expressed as

$$\ln \frac{C_t}{C_0} = -k_d t$$

where C_0 is the total amount of incorporated IAA in the hybrid at zero time of release, C_t is the total amount, and k_d is the apparent release rate constant.

(2) A parabolic diffusion equation has been used to describe diffusion-controlled phenomena in clays. The parabolic diffusion model for release may be written as follows

$$\left(1 - \frac{C_t}{C_0}\right)\frac{1}{t} = k_d t^{-0.5} + a$$

where a is a constant and k_d is the overall diffusion constant for release.

(3) A modified Freundlich model has been successfully applied to experimental data on ion exchange or adsorption with clays by many researchers. This model can be described as

$$C_0 - C_t = k_d C_0 t^a$$

where k_d is the release rate coefficient and a is a constant.

(4) An Elovich model was used to study the sorption of phosphate on clays and the sorption of NH_4^+ on zeolite. The Elovich model for release can be written as

$$1 - \frac{C_t}{C_0} = a \ln(t) + b$$

where a and b are constants but their chemical significance is not clearly resolved.

The stability of the intercalated IAA molecule in an aqueous solution was evaluated by monitoring its concentration over storage periods. The pristine IAA-ZBS hybrid (73 mg), IAA-LDH hybrid (87 mg), and pure IAA (30 mg) were separately added into the vials containing 10 mL of decarbonated water, sealed carefully with the caps, and stored in an oven with a constant temperature of 42 °C. The content of IAA was analyzed periodically with HPLC.

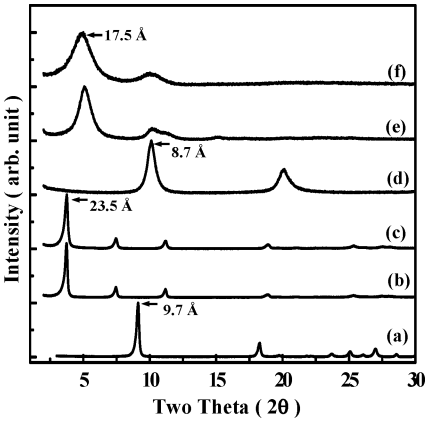

Figure 1. Powder XRD patterns of (a) ZBS, (b) IAA-ZBSI, (c) IAA-ZBSC, (d) ZALDH, (e) IAA-ZALDHI, and (f) IAA-ZALDHC.

Results and Discussion

Powder XRD Analysis. The XRD patterns of the IAA-layered metal hydroxide hybrids are represented in Figure 1, together with those of the pristine ZBS and ZALDH. Both the pristine ZBS and ZALDH show a series of well-developed (*00l*) reflections corresponding to the basal spacing of 9.7 and 8.7 Å, respectively, indicating the formation of nitrate intercalated ZBS and ZALDH phases.[12,13] After the hybridization with IAA through the coprecipitation or the ion-exchange method, the basal spacing of the pristine compounds increases markedly to 23.5 Å for ZBS and 17.5 Å for ZALDH, respectively, clearly demonstrating the intercalation of the IAA molecules into the interlayer space of layered metal hydroxide lattice. There is no distinct dependence of the crystal structure of nanohybrids on their synthetic route. The lattice expansion upon the intercalation of the IAA molecules is calculated to be greater for the ZBS compounds ($\Delta d = 13.8$ Å) than for the ZALDH compounds ($\Delta d = 8.8$ Å). This can be regarded as evidence on the different intracrystalline structure of IAA in these materials. It has been well-known that the arrangement of guest molecule in the interlayer of layered materials depends strongly on the layer charge density of layered materials and the dimension of guest species.[14,35−37] The steric limitations can be imposed by the equivalent area (A_e) of lattices of layered materials and the area demand (A_c) of intercalated molecules.[38] In the range of $A_c < A_e$, guest molecules form a monolayer arrangement parallel to the *ab*-plane. In the range of $A_e < A_c < 2A_e$, guest molecules form a parallel bilayer arrangement along the *ab*-plane because of the steric limitation. When A_c is larger than $2A_e$, intercalated molecules have a tilted bilayer arrangement with respect to the *c*-axis.

(30) Sparks, D. L. *Kinetics of Soil Chemical Processes*; Academic Press: San Diego, CA, 1989.
(31) Kithome, M.; Paul, J. W.; Lavkulich, L. M.; Bomke, A. A. *Soil Sci. Soc. Am. J.* **1998**, *62*, 622.
(32) Li, Z. *Langmuir* **1999**, *15*, 6438.
(33) Kodama, T.; Harada, Y.; Ueda, M.; Shimizu, K.; Shuto, K.; Komarneni, S. *Langmuir* **2001**, *17*, 4881.
(34) The goodness of models for the release of IAA was represented by the square of correlation coefficient (r^2). That is, as this coefficient has a higher value, the model describes more successfully the kinetics of release.
(35) Yang. J. H.; Han, Y. S.; Choy, J. H. *J. Mater. Chem.* **2001**, *11*, 1305.
(36) Meyn, M.; Beneke, K.; Lagaly, G. *Inorg. Chem.* **1990**, *29*, 5201.
(37) Costantino, U.; Coletti, N.; Nocchetti, M. *Lagmuir* **1999**, *15*, 4454.
(38) The equivalent area (A_e) of the layered materials can be estimated from the equation of $A_e = ab \sin \gamma/2\xi$, where a, b, and γ are lattice parameters and ξ is the layer charge per formula unit.

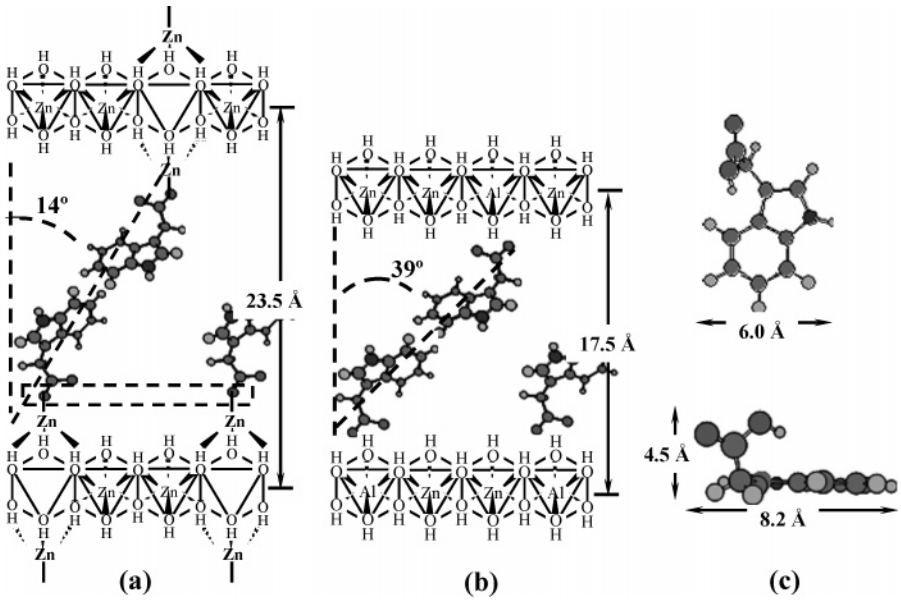

Figure 2. Interlayer arrangement model of IAA in (a) IAA-ZBS and (b) IAA-ZALDH hybrids, and (c) dimensions of the IAA obtained by Chem3D Ultra 8.0 program (CambridgeSoft). The dashed rectangle highlights coordination bonds between carbonyl groups of IAA and coordinatively unsaturated $Zn(OH)_3$ units of the ZBS lattice.

The equivalent area (A_e) for the ZBS phase with the lattice parameters of $a = 6.239$ Å, $b = 5.519$ Å, and $\gamma = 90°$ was estimated to be 8.6 Å^2.[12] On the basis of the lattice parameters and charge density of the ZALDH ($a = b = 3.076$ Å, $\gamma = 120°$; 1/3e$^-$ per unit cell),[37] we have calculated the A_e of this phase as 12.3 Å^2. On the other hand, the area demand (A_c) of the intercalated IAA molecule is about 49 Å^2, calculated from the molecular model in Figure 2c, which is lager than $2A_e$ for the pristine compounds. This calculation suggests that the bilayer of the IAA molecules would be present in the interlayer space of both the metal hydroxide lattice. From the basal increment upon the intercalation of IAA, we estimated the tilting angle of the guest molecules with respect to the *c*-axis to be 14° for the IAA-ZBS nanohybrid and 39° for the IAA-ZALDH one, as shown in Figure 2. Such a structural difference would originate from the dissimilar charge density of the pristine ZBS and ZALDH. The charge density per unit area was evaluated to be 5.8e$^-$/100 Å^2 for the former and 5.0e$^-$/100 Å^2 for the latter.[39] In this regard, ZBS layer can accommodate more anionic molecules per unit area than LDH layer, leading to more compact arrangement of guest molecules with a smaller tilting angle. As can be seen clearly from Figure 1, the ZALDH-based compounds show much broader XRD reflections than the ZBS-based ones, indicating that the particle size of the former is much smaller than that of the latter. Among the LDH-based materials, the diffraction peaks of the coprecipitated IAA-ZALDHC hybrid appear to be a little broader than those of the pristine ZALDH and the ion-exchanged IAA-ZALDHI hybrid, suggesting that the coprecipitation route causes the decrease of particle sizes and/or disorder in the stacking of hybrid layers. Previously, it was reported that ethoxide created during the coprecipitation reaction with ethanol solvent may prevent the crystal growth of LDH layer, leading to a smaller particle size.[40] Such an influence of synthetic condition on the particle size is less prominent for the ZBS-based materials, which would be related to a lower preparation pH condition for these materials unfavorable for the formation of the ethoxide. On the basis of Scherrer's equation, we have calculated the particle sizes of ZBS, IAA-ZBSI, IAA-ZBSC, ZALDH, IAA-ZALDHI, and IAA-ZALDHC as 38, 38, 31, 12, 6, and 4 nm, respectively. Because only the (00l) Bragg reflections were used for the calculations, the estimated particle size corresponds to the thickness of crystallites along the *c*-axis rather than the in-plane dimension of the crystallites.

FE-SEM Analysis. The dependence of particle sizes on the synthetic condition was cross-confirmed by FE-SEM results. As shown in Figure 3, both the pristine compounds exhibit a platelike morphology with the primary particle size of 0.3−0.5 μm for ZBS and 0.1−0.5 μm for ZALDH. Except for the IAA-LDHC hybrid with a primary particle size of less than 0.1 μm, the particle sizes of the hybrids are nearly the same as those of the corresponding pristine materials. Due to the plate-like morphology of the present materials, the particle size estimated from the FE-SEM data corresponds to the in-plane dimension of the crystallites, which is higher than the thickness calculated from the XRD data. This is in good agreement with high structural anisotropy of the layered metal hydroxides, leading to remarkable preferred orientation effects in the XRD data (Figure 1).

Thermal Analysis. Figure 4 illustrates the TGA-DTA curves of the IAA-ZBSC and the IAA-ZALDHC hybrids. The thermal decomposition of both the hybrids occurs with three steps. In the temperature region of 25−140 °C, there is an ~5−6 wt % weight loss with a broad endothermic DTA peak corresponding to the removal of adsorbed water on the surface of the hybrids and cointercalated water.[41] The second

(39) The charge density per unit area (e$^-$/100 Å^2) can be calculated from unit-cell parameters and layer charge as follows: charge density = charge × 100/(ab sin γ).

(40) Gardner, E.; Huntoon, K.M.; Pinnavaia, T. J. *Adv. Mater.* **2001**, *13* (16), 1263.

(41) Poul, L.; Jouini, N.; Fievet, F. *Chem. Mater.* **2000**, *12*, 3123.

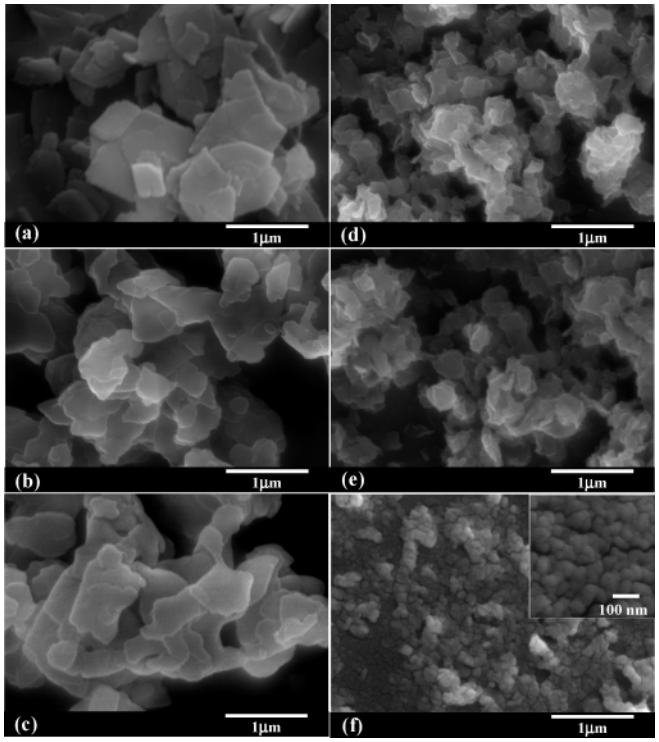

Figure 3. FE-SEM images of (a) ZBS, (b) IAA-ZBSI, (c) IAA-ZBSC, (d) ZALDH, (e) IAA-ZALDHI, and (f) IAA-ZALDHC.

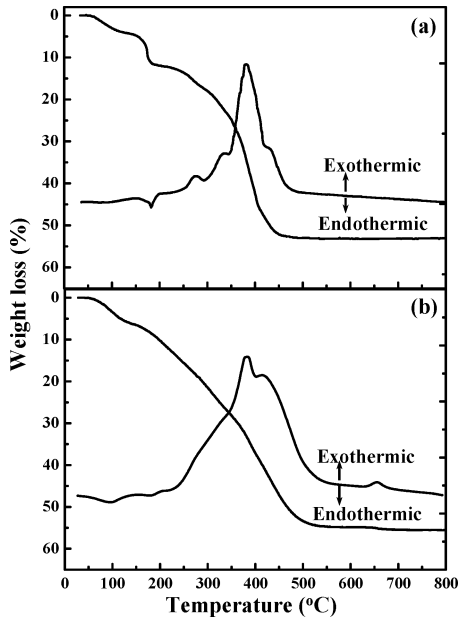

Figure 4. TGA-DTA profiles for (a) IAA-ZBSC and (b) IAA-ZALDHC hybrids.

endothermic weight loss occurs between 140 and 200 °C originates from the thermal decomposition of IAA on the surface of the crystals and the partial dehydroxylation of zinc hydroxide layer. The third weight loss between 200 and 500 °C is mainly attributable to the oxidative thermal decomposition of intercalated IAA, accompanied with the dehydroxylation of the zinc hydroxide. In the case of the IAA-LDHC hybrid, an additional weak exothermic peak is discernible at ~650 °C, which is a result of the formation of spinel $ZnAl_2O_4$ from ZnO and Al_2O_3.

FT-IR Analysis. To obtain direct evidence on the chemical interaction between IAA and host lattice, we have measured

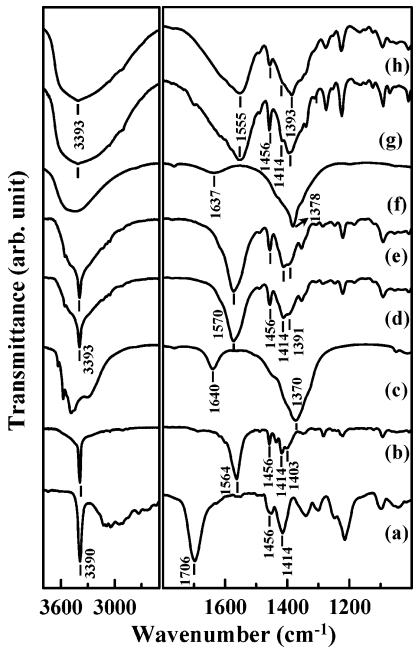

Figure 5. FT-IR spectra for (a) IAA, (b) Na^+IAA^-, (c) ZBS, (d) IAA-ZBSI, (e) IAA-ZBSC, (f) ZALDH, (g) IAA-ZALDHI, and (h) IAA-ZALDHC.

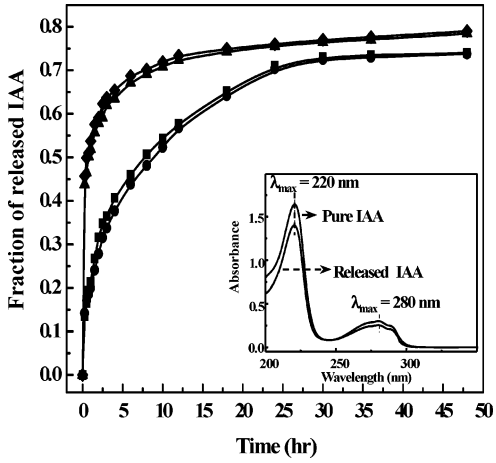

Figure 6. Time-controlled releasing profiles of IAA from IAA-ZBSI (squares), IAA-ZBSC (circles), IAA-ZALDHI (triangles), and IAA-ZALDHC (diamonds), respectively. The inset represents the UV−vis spectra of pure IAA and the guest IAA released from IAA-ZBS or IAA-ZALDH hybrids.

the FT-IR spectra of the nanohybrids, in comparison with the reference spectra of neutral IAA, sodium indole-3-acetate (Na^+IAA^-), and the pristine compounds. As shown in Figure 5, both the neutral IAA and Na^+IAA^- compounds display a very strong and sharp band at 3390 cm^{-1} corresponding to an asymmetric stretching mode of N−H bond. After the hybridization, this band is almost concealed by an intense and broad peak originating from the stretching mode of hydrogen-bonded hydroxyl groups in the host lattice at ~3390 cm^{-1}.[42] In addition, all of IAA-containing compounds exhibit two stretching bands of aromatic C═C bonds of the IAA molecules at 1456 and 1414 cm^{-1}. Before and after the hybridization, these features show no marked changes in their positions, suggesting strongly that the benzene ring

(42) Kamnev, A. A.; Shchelochkov, A. G.; Perfiliev, Yu. D.; Tarantilis, P. A.; Polissiou, M. G. *J. Mol. Struct.* **2001**, *563−564*, 565.

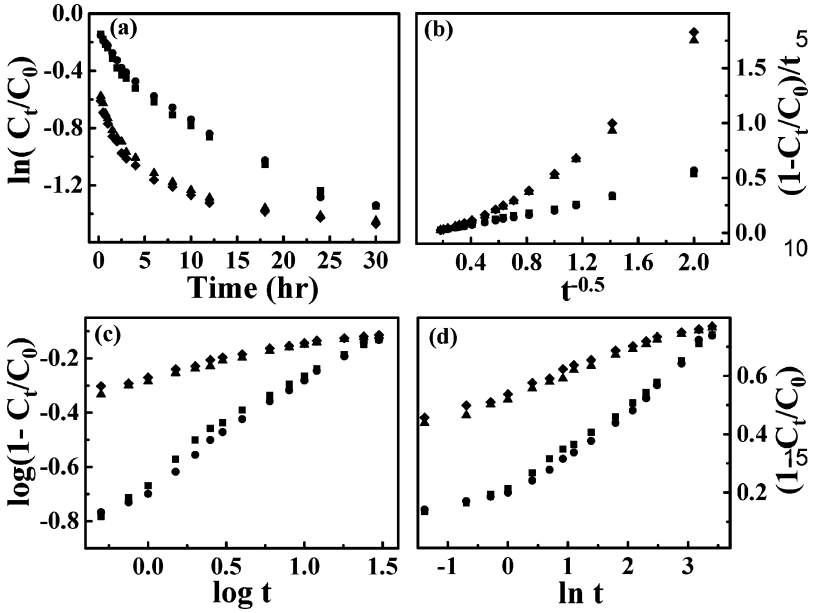

Figure 7. Plots of kinetic equations of (a) first-order kinetic model, (b) parabolic diffusion model, (c) modified Freundlich model, and (d) Elovich model for the release of IAA from IAA-ZBSI (squares), IAA-ZBSC (circles), IAA-ZALDHI (triangles), and IAA-ZALDHC (diamonds).

and indole components of the IAA molecule do not interact directly with the host metal hydroxide layers. On the contrary, an asymmetric stretching band of −COO in the neutral IAA at 1706 cm^{-1} moves markedly toward low wavenumber side upon the hybridization (1570 cm^{-1} IAA-ZBS hybrids and 1555 cm^{-1} for IAA-ZALDH hybrids). Similarly, a red-shift of this band is detected for the reference Na^+IAA^- (1564 cm^{-1}), which can be ascribed to the ionization of IAA. In addition to the low-energy shift of the asymmetric band, an additional IR band corresponding to a symmetric stretching of COO^- is observed at 1391, 1393, and 1403 cm^{-1} for ionized IAA molecules in the nanohybrids and Na^+IAA^-, respectively. This feature is absent in the spectra of neutral IAA and the pristine compounds. It has been well-documented that a wave number difference between both stretching modes of COO^-, $\Delta\nu_{as-s} = \nu_{as}(COO^-) - \nu_s(COO^-)$, becomes larger for an acetate group coordinating to metal in an unidentate way, compared to a free ionic acetate ion.[41,43,44] As can be seen from Figure 5, the $\Delta\nu$ value of IAA-ZBS hybrids (179 cm^{-1}) is greater than that of Na^+IAA^- (161 cm^{-1}), which can be regarded as strong evidence on the coordination between terminal oxygens of the guest IAA^- and exposed Zn^{2+} ions of the host ZBS lattice. On the contrary, the IAA-ZALDH hybrids show a smaller $\Delta\nu$ value of 162 cm^{-1}, which is nearly identical to the value of Na^+IAA^-. This observation clearly demonstrates negligible interaction of the guest IAA with the host LDH lattice. This is in good agreement with the previous report that the guest acetate ion has an ionic interaction with host LDH layer.[45] Of special note here is that there are no marked spectral variations depending on the synthetic methods of the nanohybrids, underscoring little influence of preparation condition on the nature of chemical bonds between the host and the guest.

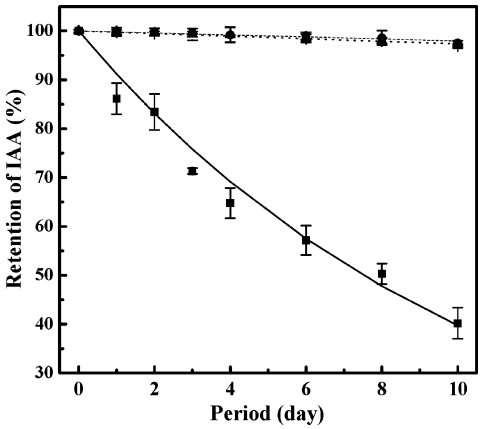

Figure 8. Retention of IAA for aqueous solution of IAA (squares) and the nanohybrids of IAA-ZBS (circles) and IAA-ZALDH (triangles) at 42 °C in aqueous medium.

Test of IAA Release Kinetics. From the present FT-IR results, it becomes certain that the guest IAA molecules can interact more strongly with the ZBS lattice than the ZALDH one. Such a different interaction would result in the dissimilar release behavior. In this respect, we have investigated the controlled release properties of IAA from the hybrids in 0.08 wt % NaCl solution. As can be seen clearly from Figure 6, a rapid release of IAA occurs at initial stage, which is followed by a slower disintercalation of the guest molecules. Such a release profile is characteristic of a diffusion-controlled release process. Regardless of the synthetic methods, both the ZBS-based materials show much slower releases of IAA than the ZALDH-based ones. In the initial period of 0.25 h, the fraction of released IAA is ∼14% for the IAA-ZBS hybrids and ∼45% for the IAA-ZALDH hybrids, respectively. More than half of the guest IAA molecules are disintercalated from the LDH lattice within 1 h, whereas the IAA-ZBS nanohybrids sustain half of the

(43) Nakamoto, K. *Infrared and Raman Spectra of Inorganic and Coordination Compounds*, 5th ed.; Wiley-Interscience; New York, 1997.
(44) Choy, J. H.; Kwon, Y. M.; Han, K. S.; Song S. W.; Chang, S. H. *Mater. Lett.* **1998**, *34*, 356.
(45) Xu, Z. P.; Zeng, H. C. *J. Phys. Chem. B* **2000**, *104*, 10206.

Table 2. Rate Constants and r^2 Coefficients Obtained from Fitting Analyses Based on Several Kinetic Equations

kinetic equation	IAA-ZBSI	IAA-ZBSC	IAA-LDHI	IAA-LDHC
First-Order $\ln(C_t/C_0) = -k_d t$				
k_d	0.0290	0.0292	0.0217	0.0212
r^2	0.842	0.862	0.605	0.579
Parabolic Diffusion Model $(1 - C_t/C_0)/t = k_d t^{-0.5} + a$				
k_d	0.270	0.280	0.880	0.922
a	−0.0336	−0.0442	−0.246	−0.260
r^2	0.999	0.977	r0.953	0.953
Modified Freundlich Model $\log(1 - C_t/C_0) = \log(k_d) + a\log(t)$				
k_d	0.228	0.219	0.525	0.545
a	0.371	0.372	0.124	0.114
r^2	0.990	0.999	0.984	0.979
Elovich Model $1 - C_t/C_0 = a\ln(t) + b$				
a	0.135	0.135	0.0742	0.0703
b	0.242	0.228	0.529	0.549
r^2	0.975	0.949	0.992	0.989

initial IAA content for longer than 7 h. To understand the release mechanism of the guest IAA, we have tried to fit the observed data to several kinetic models, as plotted in Figure 7. The rate constants and the r^2 values obtained from the best fits are given in Table 2. Among the present models, the first-order kinetic model describing dissolution phenomena gave poor r^2 values ranging from 0.58 to 0.86, suggesting that several release processes occur independently in the interlayer of host lattice. On the contrary, the parabolic diffusion model, the modified Freundlich model, and the Elovich model provided reasonable r^2 values of more than 0.95. The parabolic diffusion model describes that the release process of guest molecule by host lattice is controlled by diffusion process such as intraparticle diffusion or surface diffusion. On the other hand, the modified Freundlich model describes the release profiles from the flat surface with the heterogeneous sites by diffusion process. The Elovich model describes a number of different processes including bulk and surface diffusion, as well as activation and inactivation of catalytic surfaces.[30−33] All the calculation results suggest strongly that the release of the intercalated IAA from the hybrids is a kind of diffusion-controlled processes or heterogeneous diffusion processes. From the parabolic diffusion model, the release rate coefficients of the IAA-ZBS hybrids are determined to be ∼0.27−0.28, which are less than those of the IAA-ZALDH hybrids (∼0.88−0.92). The calculation with modified Freundlich model revealed that the release coefficients of the IAA-ZBS hybrids (∼0.22−0.23) are less than those of the IAA-ZALDH hybrids (∼0.53−0.55). There are several factors affecting the diffusion rate of the intercalated species such as a particle size of the hybrid, a chemical interaction between host and guest, and a packing density of guest species. As shown in Figure 6, both the ZALDH-based hybrids with quite different particle sizes show nearly the same release behavior of the IAA molecules, indicative of the negligible effect of crystallite size on the release rate of the guest species. On the other hand, the presence of coordinatively unsaturated $Zn(OH)_3$ units of ZBS lattice leads to the formation of a coordination bond between the exposed Zn^{2+} ions and carboxyl groups of IAA. Such a strong interaction has significant contribution to the decrease of release coefficient in the ZBS-based materials. Moreover, regardless of their synthetic methods, the ZBS-based hybrids possess higher contents of IAA than the ZALDH-based ones (Table 1) due to the higher layer charge density of the former,[16] leading to a stronger interaction between IAA molecules and a slower IAA release. In summary, a suspended release behavior of the HDS lattice can be attributed to its significant coordinative interaction between $Zn(OH)_3$ units and the guest molecules as well as to its high layer charge density.

Measurement of Chemical Stability of IAA. We have also examined the retention stability of the intercalated IAA molecules under the severe condition of elevated temperature, see Figure 8. Within 10 days, the active concentration of the free IAA molecules in aqueous solution decreases remarkably to about 40%, whereas the IAA species stabilized in the IAA-ZBS and IAA-LDH hybrids show no marked changes in concentration. Such an excellent stability of the IAA molecule in the hybrid is mainly due to an interfacial electrostatic interaction between host and guest and/or to the coordination bonds between the acetate group of IAA and the $Zn(OH)_3$ unit of the ZBS lattice.

In conclusion, we have synthesized the ZBS- and ZALDH-based IAA-containing nanohybrids, which can act not only as a drug delivery vector but also as a drug reservoir. The release rate of the guest molecules in the nanohybrids is effectively controllable by adjusting the structure type of host materials. Of special interest is that the HDS-type material like ZBS shows the suspended release rate of the guest drug molecules due not only to the higher layer charge density but also to coordinative interactions between the carboxyl groups of the guest IAA molecules and the coordinatively unsaturated $Zn(OH)_3$ units of the ZBS lattice. In this regard, the HDS-type metal hydroxide can provide a powerful route to develop new efficient DDS with suspended release rate.

Acknowledgment. This work was supported by the SRC/ERC program of the MOST/KOSEF (Grant R11-2005-008-01001-0) and partially by the financial R&D support from the SMBA (Grant S1004801).

Note Added after ASAP Publication: In the Results subsection FT-IR Analysis in the version published ASAP April 20, 2007, there was an error in a compound formula. The corrected version was published ASAP April 24, 2007.

Supporting Information Available: TGA curves and elemental CHNS data of the ZBS-and ZALDH-based nanohybrids (PDF). This material is available free of charge via the Internet at http://pubs.acs.org.

CM070259H